Dinuclear Diphosphine-Bridged Complexes of Rhodium, Iridium, and Ruthenium: Synthesis and Structure

Willi Keim,* Peter Kraneburg, Georg Dahmen, and Gregor Deckers

Institut für Technische Chemie und Petrolchemie der RWTH Aachen, Worringerweg 1, D-52074 Aachen, Germany

Ulli Englert, Klaus Linn, Thomas P. Spaniol, and Gerhard Raabe

Arbeitsgemeinschaft für Kristallographie und Strukturchemie der RWTH Aachen, Prof. Pirlet Strasse 1, D-52074 Aachen, Germany

Carl Krüger

Max-Planck-Institut für Kohlenforschung, Kaiser-Wilhelm-Platz 1, D-45470 Mülheim-Ruhr, Germany

Received June 8, 1993®

The syntheses of 25 new dinuclear diphosphine-bridged complexes of rhodium, iridium, and ruthenium with the general formula (η^n–aryl)$MCl_2R_2P(C_xH_y)_nPR_2M(\eta^n$-aryl) are reported ($\eta^n$-aryl = η^5-C_5Me_5 (Cp*), η^6-C_6Me_6 (hmb)). These complexes are examples of a rare class of compounds. To establish whether a metal–metal interaction exists, X-ray structure analyses for the following compounds were carried out: $(Cp^*IrCl_2)_2$ (μ-dmpe) (**1**), $(Cp^*RhCl_2)_2$(μ-dmpe) (**2**), $[(\eta^6\text{-}C_6Me_6)RuCl_2]_2$ (μ-dmpe) (**3**), $(Cp^*IrCl_2)_2$ (μ-dmpm) (**4**), $(Cp^*IrCl_2)_2$(μ-dmpbe) (**7**), and $[(\eta^6\text{-}C_6Me_6)RuCl_2]_2$($\mu$-dmph) (**23**). A metal–metal interaction in the solid state can be ruled out. Also, the following hydrido complexes have been synthesized: $[Cp^*Ir(H)_2]_2$-(μ-dmpe) (**24**) and $[(\eta^6\text{-}C_6Me_6)Ru(H)_2]_2$($\mu$-dmpe) (**25**). The main purpose for the syntheses of these types of complexes is the search for new routes of CH activation, the results of which will be reported in a forthcoming paper.

Introduction

There is great interest in dinuclear complexes containing bridging monodentate diphosphine ligands, as shown in Scheme 1. The well-known complexes of types A and B differ in the existence of a metal–metal bond. Many of these complexes are known.[1] In type C only one bridging diphosphine ligand is present and a metal–metal bond may exist. Examples of complexes of type C are less frequent, and most of them have been reported in the last decade. As far as we know, for type C no iridium complexes are known and only a few ruthenium and rhodium complexes, which are described below, have been reported.

Mononuclear organometallic complexes form the backbone of a great variety of industrially used homogeneous catalysts. In addition, many general concepts such as oxidative addition, reductive elimination, migratory insertion, oxidation coupling, etc. have been developed utilizing mononuclear compounds. The question arises: can the same concepts also be applied to bi- and multinuclear species, thus providing unprecedented chemical reactions and novel catalytic pathways? With this concept in mind, we initiated a program focusing on dinuclear diphosphine-bridged complexes of type C in a search for potential CH activation as shown in Scheme 2, which outlines our basic concept.

Scheme 1. Complexes with Bridging Diphosphine Ligands

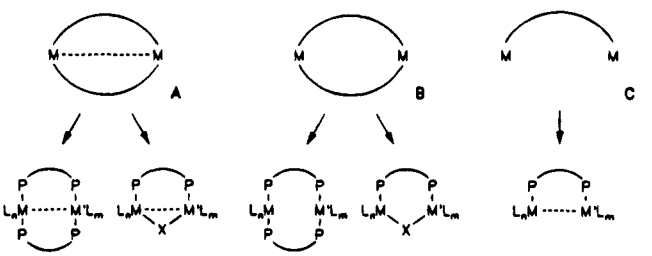

In the first step of Scheme 2, RH is oxidatively added to the two metals of C, yielding D, in which RH is activated in a discriminating fashion by the two metals. It is anticipated that by separating the two activating metal centers the reductive elimination of RH (D → C) is impeded. By this approach it may be possible to insert a further molecule X, for instance CO, yielding E. By reductive elimination of RXH the catalytic cycle will be closed. There have been many attempts to insert a molecule X into a monometallic complex with an

® Abstract published in *Advance ACS Abstracts*, June 15, 1994.

(1) (a) Jacobsen, G. B.; Shaw, B. L.; Thornton-Pett, M. *J. Chem. Soc., Chem. Commun.* **1986**, 13. (b) Cotton, F. A.; Troup, J. M. *J. Am. Chem. Soc.* **1974**, *96*, 4422. (c) Dawkins, G. M.; Green, M.; Orpen, A. G.; Stone, F. G. A. *J. Chem. Soc., Chem. Commun.* **1982**, 42. (d) Faraone, F.; Bruno, G.; Lo Schiavo, S.; Bombieri, G. *J. Chem. Soc., Dalton Trans.* **1984**, 533. (e) Sato, F.; Uemura, T.; Sato, M. *J. Organomet. Chem.* **1973**, *56*, C27. (f) Wright, M. E.; Mezza, T. M.; Nelson, G. O.; Armstrong, N. R.; Day, V. W.; Thompson, M. R. *Organometallics* **1983**, *2*, 1711. (g) Mead, K. A.; Moore, I.; Stone, F. G. A.; Woodward, P. *J. Chem. Soc., Dalton Trans.* **1983**, 2083. (h) Braunstein, P.; de Meric de Bellefon, C.; Lanfranchi, M.; Tiripicchio, A. *Organometallics* **1984**, *3*, 1772. (i) Delavaux, B.; Chaudret, B; Dahan, F.; Poiblanc, R. *Organometallics* **1985**, *4*, 935. (j) Lee, K.-W.; Pennington, W. T.; Cordes, A. W.; Brown, T. L. *J. Am. Chem. Soc.* **1985**, *107*, 631. (k) Jeffrey, J. C.; Orpen, A. G.; Stone, F. G. A.; Went, M. J. *J. Chem. Soc., Dalton Trans.* **1986**, 173. (l) Dawson, R. H.; Smith, A. K. *J. Organomet. Chem.* **1986**, *309*, C56. (m) Riera, V.; Ruiz, M. A.; Tiripicchio, A. M.; Camellini, M. T. *J. Organomet. Chem.* **1986**, *308*, C19. (n) Jacobsen, G. B.; Shaw, B. L.; Thornton-Pett, M. *J. Chem. Soc., Dalton Trans.* **1987**, 1509. (o) Azam, K. A.; Deeming, A. J.; Felix, M. S. B.; Bates, P. A.; Hursthouse, M. B. *Polyhedron* **1988**, 7, 1793.

0276-7333/94/2313-3085$04.50/0

Scheme 2. Potential CH Activation by Bimetallic Complexes

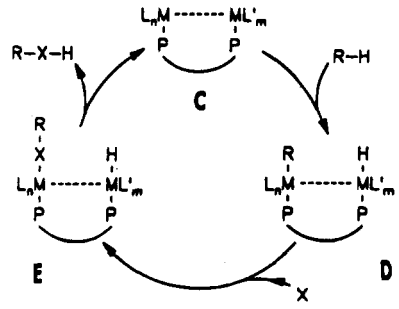

oxidatively added CH bond, but reductive elimination of RH prevailed. It was hoped that via the bimetallic approach of Scheme 2, with RH oxidatively added on two metals, reductive elimination of RH prior to insertion of X could be circumvented. Our results on activating CH bonds will be published in a separate paper.

Following Bergman's[2] and Graham's[3] pioneering work, we decided to synthesize rhodium, iridium, and ruthenium complexes of type C, as shown in Scheme 2. There are various $R_2P(CH_2)_xPR_2$ phosphine-bridged complexes of rhodium in the literature.[4] Surprisingly, to our knowledge, there are no complexes of iridium reported. Regarding ruthenium, reference must be given to Meyer,[5] Singleton,[6] and Coleman.[7] Generally it can be stated that complexes of type C are rather rare. Scheme 2 implies that the complexes proposed contain a metal–metal bond. However, complexes of type C can possess two isomeric structures, as elucidated in eq 1. In addition, type C complexes can form monometallic compounds, as also shown in eq 1.

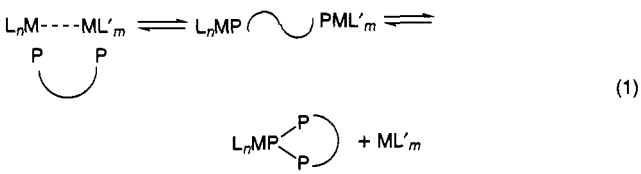

(1)

Results and Discussion

To prepare type C complexes, we systematically prepared selected dinuclear diphosphine-bridged compounds of rhodium, iridium, and ruthenium by modifying the basicity of phosphorus, the chain length, and the nature of the spacing groups between the two phosphorus atoms. Following eq 2,we could synthesize

$$[Cp^*MCl_2]_2 + R_2P(C_xH_y)_nPR_2 \rightarrow [Cp^*MCl_2]_2(\mu\text{-}R_2P(C_xH_y)_nPR_2) \quad (2)$$

19 (Table 1) new iridium (**1**, **4**–**13**) and rhodium (**2**, **14**–**20**) complexes.[8a,b] With hexamethylbenzene as starting material, paralleling eq 2, four ruthenium complexes (**3**, **18**–**20**) could be prepared.[8c]

Table 1. Ir, Rh, and Ru Complexes with $R_2P(C_xH_y)_nPR_2$ Ligands

$[Cp^*IrCl_2]_2(\mu$-dmpe) (**1**)	$[Cp^*RhCl_2]_2(\mu$-dmpm) (**14**)
$[Cp^*RhCl_2]_2(\mu$-dmpe) (**2**)	$[Cp^*RhCl_2]_2(\mu$-dmpp) (**15**)
$[(hmb)RuCl_2]_2(\mu$-dmpe) (**3**)	$[Cp^*RhCl_2]_2(\mu$-dppm) (**16**)
$[Cp^*IrCl_2]_2(\mu$-dmpm) (**4**)	$[Cp^*RhCl_2]_2(\mu$-dppp) (**17**)
$[Cp^*IrCl_2]_2(\mu$-dmpp) (**5**)	$[Cp^*RhCl_2]_2(\mu$-dppb) (**18**)
$[Cp^*IrCl_2]_2[\mu\text{-}P_2(CH_3)_4]$ (**6**)	$[Cp^*RhCl_2]_2(\mu$-dpppe) (**19**)
$[Cp^*IrCl_2]_2(\mu$-dmpbe) (**7**)	$[Cp^*RhCl_2]_2(\mu$-dpph) (**20**)
$[Cp^*IrCl_2]_2(\mu$-dppm) (**8**)	$[(hmb)RuCl_2]_2(\mu$-dmpm) (**21**)
$[Cp^*IrCl_2]_2(\mu$-dppe) (**9**)	$[(hmb)RuCl_2]_2(\mu$-dmpp) (**22**)
$[Cp^*IrCl_2]_2(\mu$-dppp) (**10**)	$[(hmb)RuCl_2]_2(\mu$-dmph) (**23**)
$[Cp^*IrCl_2]_2(\mu$-dppb) (**11**)	$[Cp^*Ir(H)_2]_2(\mu$-dmpe) (**24**)
$[Cp^*IrCl_2]_2(\mu$-dpppe) (**12**)	$[(hmb)Ru(H)_2]_2(\mu$-dmpe) (**25**)
$(Cp^*IrCl_2]_2(\mu$-dpph) (**13**)	

dmpm = $Me_2P(CH_2)PMe_2$	dppe = $Ph_2P(CH_2)_2PPh_2$
dmpe = $Me_2P(CH_2)_2PMe_2$	dppp = $Ph_2P(CH_2)_3PPh_2$
dmpp = $Me_2P(CH_2)_3PMe_2$	dppb = $Ph_2P(CH_2)_4PPh_2$
dmph = $Me_2P(CH_2)_6PMe_2$	dpppe = $Ph_2P(CH_2)_5PPh_2$
dmpbe = $Me_2P(C_6H_4)PMe_2$	dpph = $Ph_2P(CH_2)_6PPh_2$
dppm = $Ph_2P(CH_2)PPh_2$	hmb = η^6-C_6Me_6

Bis(dimethylphosphino)ethane (dmpe) Complexes of Iridium, Rhodium, and Ruthenium. The reactions of chloro-bridged dinuclear half-sandwich complexes of Ru, Rh, and Ir with 1,2-bis(dimethylphosphino)ethane (dmpe) at 0 °C in methylene chloride according to eq 2 gave in good yields (70–99%) the new dinuclear dmpe-bridged complexes $[Cp^*IrCl_2]_2(\mu$-dmpe) (**1**), $[Cp^*RhCl_2]_2(\mu$-dmpe) (**2**), and $[(hmb)RuCl_2]_2(\mu$-dmpe) (**3**).

A stoichiometric ratio of the ligand dmpe to the starting complex is important for high selectivity. A surplus of more than 10% of the ligand yields mixtures of monometallic and bimetallic complexes (see eq 1). Although the dmpe ligand itself is pyrophoric, the resulting complexes are stable in air. The yellow or red solids are soluble in chlorinated and polar solvents, from which they also can be crystallized.

Crystals of **1**–**3** suitable for X-ray structure determinations were obtained by crystallization from C_6H_5Cl, CH_2Cl_2, and $CHCl_3$ solution, respectively, covered by a *n*-pentane layer. All three complexes crystallize in the monoclinic space group $P2_1/n$ with an inversion center in the middle of the bridging diphosphine (Table 2 and Figure 1).

In $[Cp^*IrCl_2]_2(\mu$-dmpe)(**1**), as indicated by the space group symmetry, the bridging 1,2-bis(dimethylphosphino)ethane is trans and the Cp* rings are coplanar with each other. The "P–CH_2–CH_2–P backbone" of dmpe lies in a plane nearly coplanar with the Cp rings. The C–C–P angle is slightly "bent" (114.5°). The iridium–iridium distance is 7.33 Å. The bond lengths (Ir–Cl, P–C, C–C) are unexceptional and comparable to those in similar complexes.[9] The distance of iridium to the center of the Cp* ligand amounts to 1.83 Å and is shorter than in similar complexes. The Cp* rings are not significantly distorted.

In the homologous rhodium complex $[Cp^*RhCl_2]_2(\mu$-dmpe) (**2**; Figure 1), the phosphine ligand also has a

(2) (a) Janowicz, A. H.; Bergman, R. G. *J. Am. Chem. Soc.* **1982**, *104*, 352. (b) Janowicz, A. H.; Bergman, R. G. *J. Am. Chem. Soc.* **1983**, *105*, 3929. (c) Janowicz, A. H.; Periana, R. A.; Buchanan, J. M.; Kovac, C. A.; Stryker, J. M.; Wax, M. J.; Bergman, R. G. *Pure Appl. Chem.* **1984**, *56*, 12.

(3) (a) Hoyano, J. K.; Graham, W. A. G. *J. Am. Chem. Soc.* **1982**, *104*, 3723. (b) Hoyano, J. K.; McMaster, A. D.; Graham, W. A. G. *J. Am. Chem. Soc.* **1983**, *105*, 7190.

(4) Kang, J. W.; Moseley, K.; Maitlis, P. M. *J. Am. Chem. Soc.* **1969**, *91*, 5970.

(5) Sullivan, B. P.; Meyer, T. J. *Inorg. Chem.* **1980**, *19*, 752.

(6) Albers, M. O.; Liles, D. C.; Robinson, J.; Singleton, E. *Organometallics* **1987**, *6*, 2179.

(7) Coleman, A. W.; Jones, D. F.; Dixneuf, P. H.; Brisson, C.; Bonnet, J.-J.; Lavigne, G. *Inorg. Chem.* **1984**, *23*, 952.

(8) (a) Deckers, G. Dissertation, RWTH Aachen, 1987. (b) Kraneburg, P. Dissertation, RWTH Aachen, 1991. (c) Dahmen, G. Dissertation, RWTH Aachen, 1992.

(9) (a) Churchill, M. R.; Julis, S. A. *Inorg. Chem.* **1977**, *16*, 1488. (b) Stoutland, P. O.; Bergman, R. G. *J. Am. Chem. Soc.* **1988**, *110*, 5732. (c) Buchanan, J. M.; Stryker, J. M.; Bergman, R. G. *J. Am. Chem. Soc.* **1986**, *108*, 1537.

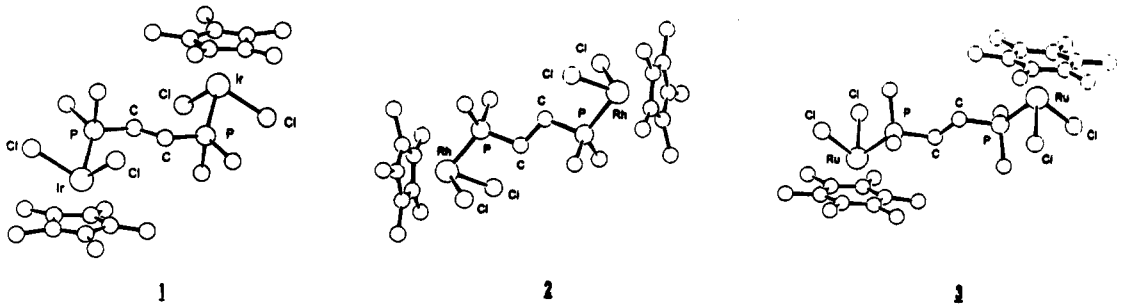

1 **2** **3**

Figure 1. Schakal plots of $[Cp^*IrCl_2]_2(\mu$-dmpe) (**1**), $[Cp^*RhCl_2]_2(\mu$-dmpe) (**2**), and $[(hmb)RuCl_2]_2(\mu$-dmpe) (**3**).

Table 2. Experimental X-ray Diffraction Data for 1–3

	$[Cp^*IrCl_2]_2(\mu$-dmpe)[a] (**1**)	$[Cp^*RhCl_2]_2(\mu$-dmpe)[b] (**2**)	$[(hmb)RuCl_2]_2(\mu$-dmpe)[c] (**3**)
mol formula	$C_{26}H_{46}Cl_4P_2Ir_2{\cdot}2C_6H_5Cl$	$C_{26}H_{46}Cl_4P_2Rh_2$	$C_{30}H_{52}Cl_4P_2Ru_2{\cdot}2CHCl_3$
mol wt	1171.9	768.2	1057.4
cryst color	orange	deep red	deep red
cryst syst	monoclinic	monoclinic	monoclinic
space group	$P2_1/n$	$P2_1/n$	$P2_1/n$
a, Å	8.295(2)	16.153(7)	9.040(1)
b, Å	18.439(6)	8.924(1)	17.025(2)
c, Å	14.389(3)	12.824(5)	14.464(3)
β, deg	91.52(2)	119.60(3)	105.80(2)
V, Å^3	2200(1)	1616(2)	2142(1)
Z	4/2	4/2	4/2
D_{calcd}, g cm^{-3}	1.77	1.58	1.64
μ, cm^{-1}	64.87	14.52	14.04
radiation	Mo Kα	Mo Kα	Mo Kα
F(000), e	908	780	1068
scan mode	ω–2θ	ω	ω-2θ
scan range, deg	$0 < \theta < 27.5$	$2.0 < \theta < 26.0$	$2.0 < \theta < 27.44$
T	room temp	room temp	room temp
no. of indep rflns	4958	3776	5064
no. of obsd rflns ($I > 2\sigma(I)$)	2840	2691	3458
no. of refined params	210	157	209
R	0.045	0.024	0.031
R_w	0.043	0.037	0.040
w	$1/\sigma^2(F_o)$	$1/\sigma^2(F_o)$	$1/\sigma^2(F_o)$
resid electron dens, e Å^{-3}	1.55	0.5	0.7

[a] Structure solved by C. Krüger, MPI Mülheim. [b] Structure solved by U. Englert, RWTH Aachen. [c] Structure solved by G. Raabe, RWTH Aachen.

Table 3. Comparison of Selected Interatomic Distances and Bond Angles for 1–3[a]

	$[Cp^*IrCl_2]_2(\mu$-dmpe) (**1**)	$[Cp^*RhCl_2]_2(\mu$-dmpe) (**2**)	$[(hmb)RuCl_2]_2(\mu$-dmpe) (**3**)
	Distances (Å)		
M–M	7.33	8.20	8.45
M–R[b]	1.83	1.81	1.72
M–C_{ring}	2.19(5)	2.17(4)	2.22(4)
M–P	2.29	2.29	2.34
M–Cl	2.43	2.41	2.42
C_{ring}–C_{ring}	1.43(5)	1.42(2)	1.42(3)
C_{ring}–C_{methyl}	1.48(3)	1.49(3)	1.51(1)
	Angles (deg)		
M–P–C_{CH_2}	118.5	111.2	115.3
P–C_{CH_2}–C_{CH_2}	114.5	115.4	115.9
C_{ring}–C_{ring}–C_{ring}	108(5)	108(2)	120(1)
C_{methyl}–C_{ring}–C_{ring}	125(3)	126(3)	120(1)

[a] Average values, variance in parentheses. [b] Middle of ring.

trans conformation but the plane of the P–C–C–P axis is arranged nearly perpendicular to the planes of the Cp* rings. The tetrahedral angle of the C–C–P bridge is also distorted to 115.4°. The metal–metal distance of 8.20 Å is significantly longer than the iridium–iridium distance in **1**. No abnormal bond distances or Cp* ring distortions were found.

Because of the d^6 configuration of Ru(II), the ruthenium in $[(hmb)RuCl_2]_2(\mu$-dmpe) (**3**; Figure 1) is bonded to the neutral six-electron-donating hexamethylbenzene ligand. Complex **3** is isoelectronic with the iridium and rhodium complexes **1** and **2**, respectively. Bond distances and angles resembled those in complexes **1** and **2**. As in complex **2**, the bridging P–C–C–P axis lies in a plane perpendicular to the hmb ring planes. At 8.45 Å the M–M distance is only 0.25 Å longer than that in the rhodium complex **2**. Table 3 compiles important interatomic distances and bond angles in complexes **1–3**. As is evident, they are all very similar despite the difference in metals.

Iridium Complexes with $R_2P(C_xH_y)_nPR_2$ Ligands. As is evident from the X-ray structure determinations of the dmpe-bridged complexes **1–3**, the two metal centers are isolated from one another and no metal–metal bonding exists in the solid state. Is it possible by modifying the diphosphine bridging ligand to force

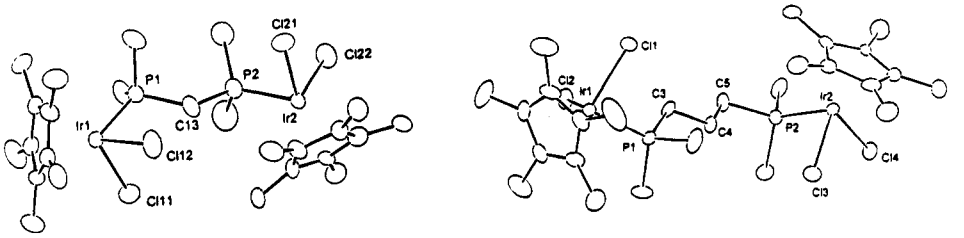

Figure 2. X-ray structures of (left) $[Cp^*IrCl_2]_2(\mu$-dmpm) (**4**) and (right) $[Cp^*IrCl_2]_2(\mu$-dmpp) (**5**).

Table 4. X-ray Diffraction Data for 4, 5, and 7[a]

	$[Cp^*IrCl_2]_2(\mu$-dmpm) (**4**)	$[Cp^*IrCl_2]_2(\mu$-dmpp) (**5**)	$[Cp^*IrCl_2]_2(\mu$-dmpbe) (**7**)
mol formula	$C_{25}H_{44}Cl_4P_2Ir_2$	$C_{27}H_{48}Cl_4P_2Ir_2$	$C_{30}H_{46}Cl_4P_2Ir_2$
mol wt	932.8	960.8	994.9
cryst color	orange	orange	red
cryst syst	tetragonal	monoclinic	triclinic
space group	*I*4	*C*2/*c*	$P\bar{1}$
a, Å	26.738(7)	32.88(1)	13.796(2)
b, Å		8.993(2)	15.390(3)
c, Å	9.123(2)	27.255(9)	8.148(1)
α, deg			91.57(1)
β, deg		123.49(3)	93.92(1)
γ, deg			99.53(1)
V, Å^3	6522(5)	6721(8)	1701(1)
Z	8	8	2
D_{calcd}, gcm^{-3}	1.93	1.90	1.94
μ, cm^{-1}	85.90	83.13	82.17
radiation	Mo Kα	Mo Kα	Mo Kα
F(000), e	3610	3696	956
scan mode	*ω*	*ω*	*ω*
scan range, deg	$2.0 < \theta < 29.0$	$3.0 < \theta < 25.0$	$3.0 < \theta < 24.0$
T, °C	20	20	20
no. of indep rflns	4492	6091	5749
no. of obsd rflns ($I > 2\sigma(I)$)	3707	3788	4177
no. of refined params	299	317	344
R	0.035	0.046	0.028
R_w ($w = 1/\sigma^2(F_o)$)	0.040	0.045	0.034
goodness of fit	1.166	1.217	1.190

[a] Structures determined by U. Englert and K. Linn, RWTH Aachen.

the two metals into a metal–metal interaction of type C as depicted Scheme 2? With this aim in mind, we synthesized the iridium complexes **4**–**13** (Table 1). Again, the reaction pathway as shown in eq 2 was chosen for their syntheses. In the dmpm complex **4** there is only one methylene group between the two phosphorus atoms, and in the dmpp complex **5** three methylene groups are spaced between the two phosphorus atoms, whereas for the Me_2PPMe_2 group in **6** only phosphorus–phosphorus bonding exists.

The NMR spectroscopic data (see Experimental Section) for the three complexes **4**–**6** are quite similar except for the bridging methylene groups. The electron donation from phosphorus to the metal leads to a high electron draw from the methylene groups. Especially in the case of **4** this deshielding effect is strong and shifts the signals downfield.

The same tendency is seen for the signals of the methyl groups of the phosphine ligands. The tetramethyldiphosphine ligand in **6** shows a very different chemical shift in the ^{31}P NMR (18.67 ppm) compared to the more basic dmpm (−16.33 ppm) and dmpp (−19.77 ppm) in **4** and **5**, respectively.

The X-ray structure determinations for **4** and **5** are detailed in Figure 2 and Table 4. Unfortunately, we were not able to obtain suitable crystals for an X-ray structure of **6**. In the dmpm complex **4** the Ir–P–C–P–Ir chain adapts an all-transoidal conformation. The P–C–P angle is opened to 127.2° to allow for maximum distance between the metal atoms with their bulky ligands. The iridium–iridium distance of 6.65 Å is 0.67 Å shorter than that of the homologous complex $[Cp^*IrCl_2]_2(\mu$-dmpe) (**1**). The pentamethylcyclopentadienyl (Cp*) ligand of Ir2 is heavily distorted by the steric interaction with the chloro atoms bonded to Ir1. It conserves planarity in the central five-membered ring, but the methyl groups are bent away from the coordinated metal atom.

Less steric influence on bonds and angles is found in $[Cp^*IrCl_2]_2(\mu$-dmpp) (**5**) (Figure 2 and Table 4). The longer chain dmpp between the two metal centers gives more flexibility, allowing intramolecular interactions to be minimized. In solution, conformational changes can be expected. In the crystal the Cp* planes are arranged perpendicular to each other. The intermetal distance of 8.42 Å is over 1 Å longer than in $[Cp^*IrCl_2]_2(\mu$-dmpe) (**1**) with 7.32 Å. It can be concluded that shortening or lengthening the $R_2P(CH_2)_nPR_2$ distances has no major impact on the structures and does not lead to a metal–metal interaction.

If the two phosphorus atoms are held in a cis conformation, as with the ligand 1,2-bis(dimethylphosphino)benzene (dmpbe), metal–metal bonding may be anticipated. For this reason, we also synthesized $[Cp^*IrCl_2]_2(\mu$-dmpbe) (**7**). In analogy to the syntheses of **1**–**6**, we obtained $[Cp^*IrCl_2]_2(\mu$-dmpe) (**7**) in a low yield of 50%. Its NMR spectroscopic data are similar to those for the other bis(dimethylphosphine)-bridged complexes. The ^{31}P NMR signal at −8.1 ppm indicates

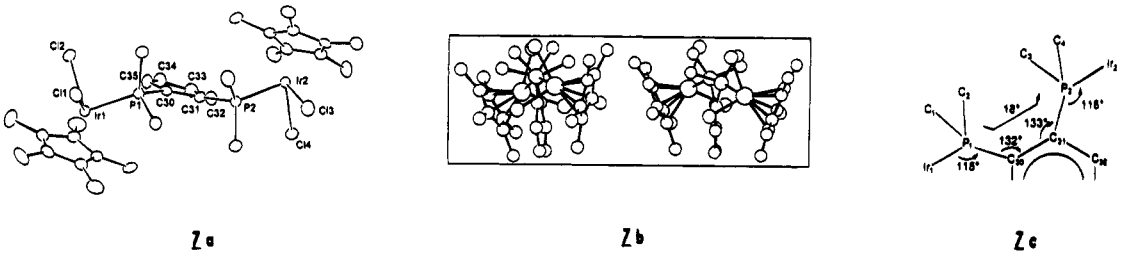

Figure 3. (a) X-ray structure of $[Cp^*IrCl_2]_2(\mu$-dmpbe) (**7**). (b) SCHAKAL plots of **7**. (c) Distortion of the backbone of **7**.

a less basic phosphine ligand compared to dmpm, dmpe, and dmpp.

The X-ray structure of **7** is given in Figure 3, which shows that there is a cis information of the P—C—C—P chain but that the iridium atoms move aside to reach a maximum distance, leading to short distances of the methyl groups of the phosphine. To avoid repulsion, the benzene ring is distorted. As shown in parts b and c of Figure 3, the aromatic ring is no longer planar and each dimethylphosphine substituent is twisted by 9° out of the "plane" of the ring. To stretch the Ir—P—C—C—P—Ir chain, the Ir—P—C_{arom} angles are bent to 115°, and the angle of the aromatic sp^2 C is widened to 132°.

Besides the methylphosphine ligands $Me_2P(C_xH_y)_n$-PMe_2, phenylphosphine ligands such as $Ph_2P(C_xH_y)_nPPh_2$ were synthesized. The homologous sequence from bis(diphenylphosphino)methane (dppm) with one methylene group up to 1,6-bis(diphenylphosphino)hexane (dpph) with six CH_2 groups gave the new complexes **8**–**13** of the general type $[Cp^*IrCl_2]_2(\mu$-$Ph_2P(CH_2)_nPPh_2)$ (Table 1). The phenylphosphines are fairly stable solids, in contrast to the methylphosphines, which are pyrophoric liquids. Because of their lower inherent reactivity, the reactions were performed at room temperature. The yields obtained vary between 80 and 95%. No phosphine-bridged complex could be obtained by reacting tetraphenylphosphine (P_2Ph_2) with $[Cp^*IrCl_2]_2$.

All complexes isolated are orange solids, quite stable to air and soluble in chlorinated solvents and moderately soluble in polar solvents such as methanol and tetrahydrofuran. All complexes were characterized unequivocally by NMR spectroscopy (Experimental Section). No evidence for iridium–iridium bonding could be found.

Rhodium Complexes with $R_2P(CH_2)_nPR_2$ Ligands. Again by the method shown in eq 2, the rhodium complexes **14**–**20** could be synthesized (Table 1). The methylphosphine complexes were obtained in yields of 85–99% and the phenylphosphine complexes in 60–90% yield. The ^1H NMR and ^{13}C NMR data (Experimental Section) for the rhodium complexes parallel those for the analogous iridium complexes. In contrast, the ^{31}P NMR data are significantly affected by changing the metal. The chemical shifts of the bis(diphenylphosphine) complexes **8**–**13** lie in the range of −1 to −6 ppm, whereas the signals of the analogous rhodium complexes **14**–**20** appear between 20 and 29 ppm. This supports the notion that the iridium complexes are more electron rich than the analogous rhodium compounds. The same holds true for the methylphosphine complexes, compared to the phenylphosphine complexes.

Ruthenium Complexes with $R_2P(CH_2)_nPR_2$ Ligands. In accordance with eq 2, the ruthenium complex $[(hmb)RuCl_2]_2$ was treated with stoichiometric amounts of dmpm, dmpp, and dmph. The diphosphine-bridged compounds **21**–**23** were obtained (Table 1). In the synthesis of the dmpm-bridged $[(hmb)RuCl_2]_2(\mu$-dmpm) (**21**), the monometallic complex $[(hmb)RuCl_2(\mu$-dmpm)] was formed, as a byproduct in a yield of ~15%. Reaction with dmpp leads to $[(hmb)RuCl_2]_2(\mu$-dmpp) (**22**), and reaction with dmph gives $[(hmb)RuCl_2]_2(\mu$-dmph) (**23**). The spectroscopic data for these three compounds are given in the Experimental Section. The electron donation of the phosphorus atoms leads to deshielding of the protons and carbon atoms of the bridging ligand, decreasing from the α- to the γ-position.

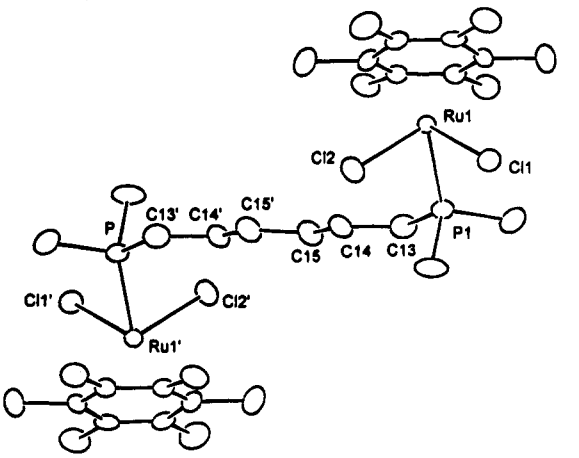

Figure 4. X-ray structure of $[(hmb)RuCl_2]_2(\mu$-dmph) (**23**).

In addition, the structure of **23** has been confirmed by X-ray structure analysis. The results are shown in Figure 4 and in Table 5. Again, the distance of the metal centers (11.323 Å) is maximized by the trans configuration of the bridging ligand. In the solid state the complex shows a crystallographic inversion center in the middle of the bridging ligand. It may be speculated that in solution the long flexible chain brings the two ruthenium metals closer together.

Hydrido Complexes $[Cp^*Ir(H)_2]_2(\mu$-dmpe) (24) and $[hmbRu(H)_2]_2(\mu$-dmpe) (25). The chloro complexes **1** and **3** were converted to the corresponding hydrido complexes $[Cp^*Ir(H)_2(\mu$-dmpe) (**24**) and $[(hmb)$-$Ru(H)_2]_2(\mu$-dmpe) (**25**) via reaction with $Li(Et_3BH)$ and $NaBH_4$, respectively. The resulting hydrides **24** and **25** are extremely sensitive to moisture and air. No crystals suitable for X-ray structure analyses could be obtained. Therefore, they could be characterized only spectroscopically. The iridium complex **24** showed the expected ^1H NMR signal at −17.57 ppm as a doublet resulting from a $^2J_{HP}$ coupling of 31 Hz. The IR spectrum shows strong iridium–hydride bonds at 2115 and 2086 cm^{-1}. The ^1H NMR spectrum for $[(hmb)Ru(H)_2]_2(\mu$-dmpe) (**25**) gives the hydride resonance at −11.1 ppm. The IR spectrum shows two strong $Ru(H)_2$ bands at 1928 and 1895 cm^{-1}. For detailed spectroscopic data and elemental analyses, see the Experimental Section.

Table 5. X-ray Diffraction Data for [(hmb)$RuCl_2$]$_2$(μ-dmph)·3$CHCl_3$ (23)[a]

mol formula	$C_{34}H_{60}Cl_4P_2Ru_2 \cdot 3CHCl_3$
mol wt	1232.9
cryst color	red
cryst syst	triclinic
space group	$P\bar{1}$
a, Å	9.070(6)
b, Å	16.287(5)
c, Å	19.024(7)
a, deg	106.47(3)
β, deg	96.90(4)
γ, deg	97.41(1)
V, Å^3	1701(4)
Z	2
D_{calcd}, g cm^{-3}	1.55
μ, cm^{-1}	13.14
radiation	Mo Kα
F(000), e	1248
diffractometer	Enraf-Nonius
scan mode	Ω
scan range, deg	$3.0 < \theta < 22.0$
T, °C	20
no. of indep rflns	6927
no. of obsd rflns ($I > 3\sigma(I)$)	5203
no. of refined params	515
R	0.060
R_w ($w = 1/\sigma^2(F_o)$)	0.060
goodness of fit	2.016
resid electron dens, e Å^{-3}	0.67 (1.28 Å away from Ru_1)

[a] Structure determined by T. P. Spaniol, RWTH Aachen.

Conclusions

A series of new $R_2P(C_xH_y)_nPR_2$ diphosphine-bridged complexes of rhodium, iridium, and ruthenium of the type C shown in Scheme 1 could be synthesized. X-ray structure determinations confirm that in the crystalline state neither lengthening nor shortening the $P(C_xH_y)_nP$ chain induces a metal–metal bond to exist. This does not rule out that in solution a metal–metal interaction may exist. With Scheme 2 in mind these complexes were used to activate C–H bonds. The results will appear in a separate paper.

Experimental Section

General Information. All experiments were carried out in Schlenk type glassware under argon and with solvents that were thoroughly dried and deoxygenated. $IrCl_3 \cdot xH_2O$, $RhCl_3 \cdot xH_2O$, and $RuCl_3 \cdot xH_2O$ were from Degussa AG, Frankfurt, Germany. [Cp*$IrCl_2$]$_2$[10] [Cp*$RhCl_2$]$_2$,[11] and [(hmb)$RuCl_2$]$_2$[12] were prepared as described in the literature. 1,2-Bis(dimethylphosphino)ethane (dmpe) was prepared from 1,2-bis(dichlorophosphino)ethane[13] and the Grignard compound CH_3MgI. The bis(dimethylphosphines) are synthesized by a general method using tetramethyldiphosphines.[14] The Na[$P(CH_3)_2$] reagent was obtained in situ by P–P bond cleavage with sodium (in liquid NH_3; −78 °C); reaction with different α,ω-dichlorohydrocarbons gave bis(dimethylphosphines such as dmpp. It was reported that synthesis of $P_2(CH_3)_4$ led to an accident;[15] therefore, care has to be taken. Bis(dimethylphosphino)methane (dmpm) was synthesized via the dialuminum compound $Cl_2AlCH_2AlCl_2$.[16] To synthesize dmpbe, 1,2-difluorobenzene was used instead of 1,2-dichlorobenzene, which gave no product. The yield was only 7%. The phenylphosphines were commercially available from Aldrich and Fluka.

NMR spectra were recorded on a Bruker CXP 200 spectrometer; the samples were sealed in NMR tubes, and the signal of the solvent was used as an internal reference (^{1}H, ^{13}C), or 85% phosphoric acid was used as an external standard (^{31}P). Chemical shifts are reported on the δ scale. IR spectra were recorded as KBr pellets on a Perkin-Elmer PE 782 spectrometer. Microanalyses were performed on a Carlo Erba 1106 CHN analyzer. Satisfactory analyses could not be obtained for compounds **9-11** and **13-25** due to solvent inclusion. Spectroscopic data, however, are unequivocal. X-ray data were collected on an Enraf-Nonius CAD4 diffractometer.

General Method for Synthesis of Complexes. In a solution of 6 mmol of [(η^n-aryl)MCl_2]$_2$ (M = Ir, Rh) in 150 mL of CH_2Cl_2, a solution of 6 mmol of the diphosphine in 180 mL of CH_2Cl_2 is dropped over 1 h at 0 °C (for methylphosphine ligands) or at room temperature (for phenylphosphine ligands). The orange-red solutions are stirred for 18 h. A 120-mL amount of the solvent is evaporated, and when 100 mL of n-pentane is added, orange or red solids precipitate which are isolated by filtration. Slow crystallization may be achieved by a careful layering of a CH_2Cl_2 solution with n-pentane. This led to products of high purity.

[Cp*$IrCl_2$]$_2$(μ-dmpe) (1). To a solution of 4.78 g (6 mmol) of [Cp*$IrCl_2$]$_2$ in 150 mL of CH_2Cl_2 was added a mixture of 0.9 g (6 mmol) of dmpe and 180 mL of CH_2Cl_2 slowly over 1 h at 0 °C. The orange solution was stirred for 18 h; it was warmed slowly to room temperature. The solvent was reduced in volume to about 60 mL. When 10 mL of n-pentane was added, a yellow-orange solid precipitated, which was filtered off. The complex was recrystallized from CH_2Cl_2/n-pentane, yielding 5.62 g (5.9 mmol) of complex **1** (yield 99%). Anal. Calcd for $C_{26}H_{46}Cl_4Ir_2P_2$: C, 32.98; H, 4.90. Found: C, 32.16; H, 4.70. The X-ray structure is given in Figure 1. IR (ν, cm^{-1}): 2979, 2964, 2915, 1640, 1502, 1450, 1376, 1294, 1280, 1190, 1155, 1104, 1078, 1029, 945, 910, 841, 800, 740, 697, 672, 430. For NMR data, see Table 6. Table 7 gives the fractional coordinates.

[Cp*RhCl$_2$]$_2$(μ-dmpe) (2). By the procedure used to prepare **1**, with 6 mmol of [Cp*$RhCl_2$]$_2$ and 4.53 g (5.1 mmol) of dmpe as starting materials, complex **2** was obtained as a deep red solid. The yield is about 85% after recrystallization. Anal. Calcd for $C_{26}H_{46}Cl_4P_2Rh_2$: C, 40.65; H, 6.04. Found: C, 39.76; H, 5.83. For NMR data, see Table 6. IR (ν, cm^{-1}): 2979, 2964, 2915, 1640, 1502, 1450, 1376, 1294, 1280, 1190, 1155, 1104, 1078, 1029, 945, 910, 841, 800, 740, 697, 672, 430. The X-ray structure is shown in Figure 1. Table 8 gives the data obtained for the fractional coordinates.

[(hmb)$RuCl_2$]$_2$(μ-dmpe) (3). Chloroform is used as the solvent for the synthesis of **3**. A mixture of 0.9 g (6 mmol) of dmpe in 80 mL of $CHCl_3$ is slowly added to a solution of 6 mmol of [(hmb)$RuCl_2$]$_2$ in 250 mL of $CHCl_3$. Otherwise the same procedure as for **1** and **2** is followed. After recrystallization from $CHCl_3$/n-pentane, [(hmb)$RuCl_2$]$_2$(μ-dmpe) is obtained in 70% yield as red crystals. Anal. Calcd for $C_{30}H_{52}Cl_4P_2Ru_2 \cdot 2CHCl_3$: C, 36.35; H, 5.15; Cl, 5.86; P, 33.53. Found: C, 36.09; H, 5.08; Cl, 6.14; P, 33.73. For NMR data, see Table 6. IR (ν, cm^{-1}): 3010, 2970, 2920, 2860, 2480, 1960, 1925, 1640, 1420, 1382, 1290, 1280, 1245, 1180, 1105, 1070, 1015, 945, 905, 845, 835, 800, 750, 745, 690, 670, 660, 545,

(10) Brauer, G. *Handbuch der Präparativen Anorganischen Chemie*; Ferdinand Enke Verlag: Stuttgart, Germany, 1981.
(11) (a) Churchill, M. R.; Julis, S. A. *Inorg. Chem.* **1977**, *16*, 1488. (b) Stoutland, P. O.; Bergman, R. G. *J. Am. Chem. Soc.* **1988**, *110*, 5732. (c) Buchanan, J. M.; Stryker, J. M.; Bergman, R. G. *J. Am. Chem. Soc.* **1986**, *108*, 1537.
(12) Bennett, M. A.; Huang, T. N.; Matheson, T. W.; Smith, A. K. *Inorg. Synth.* **1982**, *21*, 74.
(13) Burt, R. J.; Chatt, J.; Hussain, W.; Leigh, G. J. *J. Organomet. Chem.* **1979**, *182*, 203.
(14) (a) Parshall, G. W. *Org. Synth.* **1965**, *45*, 102. (b) Kordosky, G.; Cook, B. R.; Cloyd, J., Jr.; Meek, D. W. *Inorg. Synth.* **1974**, *14*, 14.
(15) (a) Bercaw, J. E. *Chem. Eng. News* **1984**, *62*, 4. (b) Bercaw, J. E.; Parshall, G. W. *Inorg. Synth.* **1985**, *23*, 199.
(16) (a) Novikova, Z. S.; Prishchenko, A. A.; Lutsenko, I. F. *Zh. Obshch. Khim.* **1977**, *47*, 775. (b) Hietkamp, S.; Stelzer, O. *Chem. Ber.* **1984**, *117*, 3409. (c) Schmidbaur, H.; Schnatterer, S. *Chem. Ber.* **1986**, *119*, 2832.

Table 6. NMR Spectra Data (δ, ppm) for 1–3

signal	$[Cp^*IrCl_2]_2(\mu$-dmpe) (1)	$[Cp^*RhCl_2]_2(\mu$-dmpe) (2)	$[(hmb)RuCl_2]_2(\mu$-dmpe) (3)
		^1H NMR	
CH_3—ring	1.67 (x)[b]	1.62 (d)	2.03 (s)[c]
CH_3—P	1.63 (x)	1.53 (d)	1.44 (x)
CH_2—P	2.26 (d)	2.23 (d)	2.03 (s)[c]
		$^{13}C(^1H)$NMR	
CH_3—ring	9.09 (s)	9.29 (s)	16.02 (s)
C ring	91.56 (s)	98.35 (d)	95.54 (s)
CH_3—P	11.35 (dd)	11.78 (x)	12.03 (d)
CH_2—P	22.56 (dd)	22.91 (x)	22.73 (d)
		$^{31}P(^1H)$ NMR	
P	−19.17 (s)	16.00 (dt)	9.41 (s)

[a] Solvent $CDCl_3$. [b] x = no first-order coupling. [c] Signals fall together.

Table 7. Fractional Coordinates for $[Cp^*IrCl_2]_2(\mu$-dmpe) (1)

atom	x	y	z
Ir	0.1259(1)	0.1719(1)	0.1069(1)
Cl1	0.3098(4)	0.1631(2)	−0.0207(2)
Cl2	0.3496(3)	0.1706(2)	0.2189(2)
P	0.1377(3)	0.0484(2)	0.12224(2)
Cp1	−0.076(1)	0.2219(7)	0.0327(9)
Cp2	0.033(1)	0.2805(6)	0.0618(9)
Cp3	0.039(1)	0.2797(7)	0.1579(9)
Cp4	−0.049(1)	0.2212(7)	0.1945(8)
Cp5	−0.133(1)	0.1871(6)	0.1141(8)
C1	−0.133(2)	0.2092(9)	−0.064(1)
C2	0.104(2)	0.3338(9)	−0.002(1)
C3a	0.1530	0.3331	0.2068
C3b	0.1164	0.3256	0.2336
C4	−0.079(2)	0.2062(9)	0.292(1)
C5	−0.264(1)	0.1330(8)	0.118(1)
C6	−0.002(1)	−0.0078(7)	0.0502
C7	0.098(1)	0.0177(7)	0.2394(9)
C8	0.333(1)	0.0073(7)	0.098(1)

Table 8. Fractional Coordinates and Thermal Parameters for $[Cp^*RhCl_2]_2(\mu$-dmpe) (2)

atom	x	y	z	B (Å^2)[a]
Rh	0.46753(1)	0.21456(2)	0.22699(2)	2.816(4)
Cl1	0.36585(6)	0.1402(1)	0.02102(7)	4.67(2)
Cl2	0.38873(5)	0.44827(9)	0.21166(6)	4.46(2)
P	0.55355(4)	0.34522(9)	0.15927(6)	2.98(1)
Cp1	0.5813(2)	0.0849(3)	0.3666(2)	3.52(6)
C1	0.6839(2)	0.0703(5)	0.3979(3)	6.3(1)
Cp2	0.5070(2)	−0.0098(3)	0.2891(3)	4.20(8)
C2	0.5149(4)	−0.1348(5)	0.2202(4)	8.5(2)
Cp3	0.4243(2)	0.0238(4)	0.2981(3)	6.17(9)
C3	0.3314(3)	−0.0527(6)	0.2348(5)	13.8(2)
Cp4	0.4498(2)	0.1436(5)	0.3797(3)	7.44(8)
C4	0.3872(3)	0.2206(7)	0.4212(4)	14.2(1)
Cp5	0.5459(3)	0.1881(4)	0.4183(3)	4.75(8)
C5	0.6008(5)	0.3048(5)	0.5069(3)	10.0(2)
C6	0.4752(2)	0.4496(4)	0.0227(2)	4.17(7)
C7	0.6339(2)	0.4824(4)	0.2650(3)	4.90(9)
C8	0.6291(2)	0.2361(4)	0.1215(3)	5.58(8)

[a] Anistropically refined atoms are given in the form of th isotropic equivalent displacement paramaters defined as $^4/_3[a^2\beta(1,1) + b^2\beta(2,2) + c^2\beta(3,3) + ac(\cos 119.6°)\beta(1,3)]$.

530, 450, 410. The X-ray structure is shown in Figure 1. Table 9 lists the data obtained for the fractional coordinates.

$[Cp^*IrCl_2]_2(\mu$-dmpm) (4). A 6-mmol (5.6-g) amount of $[Cp^*IrCl_2]_2$ was reacted with a solution of 6 mmol (0.82 g) of dmpm in 180 mL of CH_2Cl_2. The reaction was carried out at 0 °C. The complex was isolated in a yield of 99%. Anal. Calcd. for $C_{25}H_{44}Cl_4P_2Ir_2$: C, 31.19; H, 4.75. Found: C, 31.06; H, 4.55. For NMR data, see Table 10. See ref 17 regarding IR data.

(17) No unusual or informative bands. Data are available from the author on request, or see ref 8.

Table 9. Fractional Coordinates and Thermal Parameters for $[(hmb)RuCl_2]_2(\mu$-dmpe) (3)

atom	x	y	z	B (Å^2)[a]
Ru	0.65898(3)	0.89681(2)	0.77339(2)	1.97(2)
Cl1	0.4251(1)	0.90559(6)	0.82310(8)	3.53(4)
Cl2	0.7237(1)	0.77865(6)	0.86866(7)	3.63(4)
P	0.7576(1)	0.96324(6)	0.91831(7)	2.41(3)
C1	0.5664(5)	0.9708(2)	0.6476(3)	3.5(2)
C2	0.5123(4)	0.8927(3)	0.6198(3)	3.3(2)
C3	0.6150(4)	0.8305(2)	0.6341(3)	2.9(2)
C4	0.7753(4)	0.8447(2)	0.6712(3)	2.8(2)
C5	0.8318(4)	0.9216(2)	0.6922(3)	2.9(2)
C6	0.7265(5)	0.9855(2)	0.6814(3)	3.2(2)
C7	0.4507(7)	1.0365(3)	0.6364(4)	6.3(2)
C8	0.3418(5)	0.8778(4)	0.5811(4)	5.8(2)
C9	0.5562(6)	0.7467(3)	0.6135(3)	4.7(2)
C10	0.8866(5)	0.7770(3)	0.6854(3)	4.4(2)
C11	1.0031(5)	0.9362(3)	0.7200(3)	4.6(2)
C12	0.7853(7)	1.0682(3)	0.7002(4)	5.2(2)
C13	0.9669(4)	0.9794(2)	0.9525(3)	3.2(2)
C14	0.7256(5)	0.9175(3)	1.0245(3)	3.6(2)
C15	0.6774(5)	1.0606(2)	0.9212(3)	3.9(2)

[a] Anisotropically refined atoms are given in the form of the isotropic equivalent displacement parameters defined as $^4/_3[a^2\beta(1,1) + b^2\beta(2,2) + c^2\beta(3,3) + ac(\cos 105.8°)\beta(1,3)]$.

The X-ray structure is shown in Figure 2. Table 11 lists the data obtained for the fractional coordinates.

$[Cp^*IrCl_2]_2(\mu$-dmpp) (5). A 6-mmol (5.6-g) amount of $[Cp^*IrCl_2]_2$ was reacted with a solution of 6 mmol (0.98 g) of dmpp in 180 mmol of CH_2Cl_2. The reaction was carried out at 0 °C. The complex was isolated in a yield of 94%. Anal. Calcd for $C_{27}H_{48}Cl_4P_2Ir_2$: C, 33.75; H, 4.78. Found: C, 32.81; H, 5.04. For NMR data, see Table 10. See ref 17 regarding IR data. The X-ray structure is shown in Figure 2. Table 12 lists the data obtained for the fractional coordinates.

$[Cp^*IrCl_2]_2(\mu$-P_2Me_4) (6). A 6-mmol (5.6-g) amount of $[Cp^*IrCl_2]_2$ was reacted with a solution of 6 mmol (0.73 g) of Me_2PPMe_2 in 180 mL of CH_2Cl_2. The reaction was carried out at 0 °C. The complex was isolated in a yield of 91%. Anal. Calcd for $C_{24}H_{42}Cl_4P_2Ir_2$: C, 31.38; H, 4.61. Found: C, 30.76; H, 4.37. For NMR data, see Table 10. See ref 17 regarding IR data.

$[Cp^*IrCl_2]_2(\mu$-dmpbe) (7). A 6-mmol (5.6-g) amount of $[Cp^*IrCl_2]_2$ was reacted with a solution of 6 mmol (1.19 g) of dmpbe in 180 mL of CH_2Cl_2. The reaction was carried out at 0 °C. The complex was isolated in a yield of 49%. Anal. Calcd for $C_{30}H_{46}Cl_4P_2Ir_2$: C, 36.22; H, 4.66. Found: C, 35.24; H, 4.60. For NMR data see Tables 13 and 14. See ref 17 regarding IR data. The X-ray structure is given in Figure 3; Table 15 lists the fractional coordinates.

$[Cp^*IrCl_2]_2(\mu$-dppm) (8). A 6-mmol (5.6-g) amount of $[Cp^*IrCl_2]_2$ was reacted with a solution of 6 mmol (2.30 g) of dppm in 180 mL of CH_2Cl_2. The reaction was carried out at room temperature. The complex was isolated in a yield of 94%. Anal. Calcd for $C_{45}H_{52}Cl_4P_2Ir_2$: C, 45.76; H, 4.44. Found: C, 44.50; H, 4.38. For NMR data, see Tables 13 and 14. See ref 17 regarding IR data.

Table 10. NMR Spectroscopic Data (δ, ppm) for 4–6 (in $CDCl_3$)

signal	$[Cp^*IrCl_2]_2(\mu\text{-}P_2(CH_3)_4$ (6)	$[Cp^*IrCl_2]_2(\mu$-dmpm) (4)	$[Cp^*IrCl_2]_2(\mu$-dmpp) (5)
		^1H NMR	
CH_3—ring	1.75 (x)[a]	1.67 (x)	1.67 (d)
CH_3—P	2.28 (dd)	1.88 (x)	1.62 (d)
CH_2—P		3.10 (t)	2.09 (m)
CH_2CH_2—P			1.82 (m)
		$^{13}C\{^1H\}$ NMR	
CH_3—ring	9.08 (s)	9.00 (s)	8.87 (s)
C ring	93.45 (s)	91.57 (s)	91.13 (s)
CH_3—P	13.62 (dd)	13.35 (dd)	11.04 (d)
CH_2—P		23.87 (t)	28.76 (dd)
CH_2CH_2—P			17.86 (s)
		$^{31}P\{^1H\}$ NMR	
P	18.67 (s)	−16.33 (s)	−19.77 (s)

[a] x = no first-order coupling.

Table 11. Fractional Coordinates and Thermal Parameters for $[Cp^*IrCl_2]_2(\mu$-dmpm) (4)

atom	x	y	z	B (Å^2)[a]
Ir1	0.67174(1)	0.48341(1)	0.21416(5)	1.924(5)
Ir2	0.83972(2)	0.32970(1)	−0.07989(5)	2.096(7)
Cl11	0.6795(1)	0.4924(1)	−0.0478(3)	3.75(7)
Cl12	0.6610(1)	0.3953(1)	0.1816(5)	4.06(8)
Cl21	0.8420(1)	0.3007(1)	0.1708(4)	3.83(7)
Cl22	0.9295(1)	0.3393(1)	−0.0875(5)	4.20(7)
P1	0.7567(1)	0.4728(1)	0.2113(4)	2.31(5)
P2	0.8372(1)	0.4093(1)	0.0145(4)	2.73(6)
C1	0.6664(4)	0.5336(4)	0.404(1)	2.8(2)
C2	0.6485(5)	0.5579(4)	0.274(1)	2.7(2)
C3	0.6035(4)	0.5317(4)	0.226(1)	2.3(2)
C4	0.5960(4)	0.4905(4)	0.320(1)	2.4(2)
C5	0.6366(4)	0.4891(4)	0.425(1)	2.5(2)
C6	0.7052(5)	0.5537(5)	0.509(2)	4.4(3)
C7	0.6671(5)	0.6058(4)	0.209(2)	3.9(3)
C8	0.5720(5)	0.5464(5)	0.099(2)	3.5(3)
C9	0.5560(5)	0.4527(5)	0.312(2)	3.9(3)
C10	0.6403(6)	0.4544(5)	0.552(2)	4.3(3)
C11	0.7920(4)	0.5282(4)	0.156(2)	3.6(3)
C12	0.7852(6)	0.4548(5)	0.387(2)	5.1(3)
C13	0.7749(4)	0.4217(4)	0.090(2)	3.0(2)
C14	0.8832(5)	0.4213(5)	0.161(2)	4.3(3)
C15	0.8487(6)	0.4574(6)	−0.115(2)	5.2(4)
C20	0.7006(4)	0.7670(4)	0.138(1)	2.8(2)
C21	0.7426(4)	0.8042(4)	0.158(1)	2.7(2)
C22	0.7267(5)	0.8392(5)	0.264(1)	3.0(2)
C23	0.6751(4)	0.8263(5)	0.309(1)	3.2(2)
C24	0.6635(4)	0.7795(5)	0.238(1)	2.8(2)
C25	0.7075(5)	0.7225(4)	0.043(2)	3.3(3)
C26	0.7909(4)	0.8016(5)	0.076(2)	3.5(3)
C27	0.7569(4)	0.8827(4)	0.323(1)	3.0(2)
C28	0.6463(5)	0.8556(6)	0.433(2)	4.6(3)
C29	0.6194(4)	0.7471(4)	0.280(2)	3.5(2)

[a] Anisotropically refined atoms are given in the form of the isotropic equivalent displacement parameters defined as $^4/_3[a^2\beta(1,1) + b^2\beta(2,2) + c^2\beta(3,3)]$.

Table 12. Fractional Coordinates and Thermal Parameters for $[Cp^*IrCl_2]_2(\mu$-dmpp) (5)

atom	x	y	z	B (Å^2)[a]
Ir1	0.14166(1)	0.02030(5)	0.25753(2)	2.02(1)
Ir2	0.10205(1)	−0.46899(5)	0.49150(2)	2.006(9)
Cl1	0.1890(1)	0.0949(4)	0.3597(1)	3.28(8)
Cl2	0.1973(1)	−0.1766(4)	0.2741(1)	3.64(8)
Cl3	0.0304(1)	−0.4323(4)	0.3942(1)	3.97(9)
Cl4	0.0734(1)	−0.7144(4)	0.4937(1)	3.65(8)
P1	0.1058(1)	−0.1476(4)	0.2857(1)	2.31(7)
P2	0.1385(1)	−0.5869(4)	0.4511(1)	2.43(7)
C1	0.0682(4)	−0.067(2)	0.3078(5)	4.6(4)
C2	0.0658(5)	−0.277(2)	0.2284(6)	4.5(4)
C3	0.1490(4)	−0.264(1)	0.3481(5)	3.0(3)
C4	0.1263(4)	−0.366(1)	0.3709(4)	2.6(3)
C5	0.1630(4)	−0.471(1)	0.4186(4)	2.9(3)
C6	0.1894(4)	−0.705(2)	0.5019(6)	4.0(4)
C7	0.0983(4)	0.711(2)	0.3900(5)	4.1(4)
C10	0.1114(4)	0.043(2)	0.1653(5)	3.4(3)
C11	0.0773(4)	0.102(2)	0.1777(5)	3.4(4)
C12	0.1019(5)	0.221(2)	0.2170(5)	3.8(4)
C_{13}	0.1473(6)	0.243(2)	0.2263(6)	5.2(5)
C14	0.1550(4)	0.133(2)	0.1952(5)	4.0(3)
C15	0.1012(5)	−0.081(2)	0.1231(6)	5.8(5)
C16	0.0248(4)	0.067(2)	0.1472(6)	5.0(4)
C17	0.0776(7)	0.324(2)	0.2389(7)	8.1(6)
C18	0.1854(6)	0.359(2)	0.2649(7)	7.6(6)
C19	0.1972(4)	0.110(2)	0.1893(7)	6.6(5)
C20	0.1028(4)	−0.399(2)	0.5709(5)	3.0(3)
C21	0.1502(3)	−0.432(1)	0.5833(4)	2.2(3)
C22	0.1619(4)	−0.327(1)	0.5530(4)	2.6(3)
C23	0.1195(4)	−0.241(1)	0.5164(5)	2.8(3)
C24	0.0831(4)	−0.280(1)	0.5292(6)	3.5(4)
C25	0.0771(4)	−0.476(2)	0.5946(5)	4.8(4)
C26	0.1849(5)	−0.540(2)	0.6307(6)	5.1(4)
C27	0.2110(4)	−0.306(1)	0.5625(5)	3.3(4)
C28	0.1148(5)	−0.110(1)	0.4806(6)	4.3(4)
C29	0.0334(4)	−0.212(2)	0.5010(6)	5.0(4)

[a] Anisotropically refined atoms are given in the form of the isotropic equivalent displacement parameters defined as $^4/_3[a^2\beta(1,1) + b^2\beta(2,2) + c^2\beta(3,3) + ac(\cos 123.49°)\beta(1,3)]$.

$[Cp^*IrCl_2]_2(\mu$-dppe) (9). A 6-mmol (5.6-g) amount of $[Cp^*IrCl_2]_2$ reacted with a solution of 6 mmol (2.39 g) of dppe in 180 mL of CH_2Cl_2. The reaction was carried out at room temperature. The complex was isolated in a yield of 91%. For NMR data, see Tables 13 and 14. See ref 17 regarding IR data.

$[Cp^*IrCl_2]_2(\mu$-dppp) (10). A 6-mmol (5.6-g) amount of $[Cp^*IrCl_2]_2$ was reacted with a solution of 6 mmol (2.47 g) of dppp in 180 mL of CH_2Cl_2. The reaction was carried out at room temperature. The complex was isolated in a yield of 82%. For NMR data, see Tables 13 and 14. See ref 17 regarding IR data. **$[Cp^*IrCl_2]_2(\mu$-dppb) (11).** A 6-mmol (5.6-g) amount of $[Cp^*IrCl_2]_2$ was reacted with a solution of 6 mmol (2.56 g) of dppb in 180 mL of CH_2Cl_2. The reaction was carried out at room temperature. The complex was isolated in a yield of 94%. For NMR data, see Tables 13 and 14. See ref 17 regarding IR data.

$[Cp^*IrCl_2]_2(\mu$-dppe) (12). A 6-mmol (5.6-g) amount of $[Cp^*IrCl_2]_2$ was reacted with a solution of 6 mmol (2.64 g) of dpppe in 180 mL of CH_2Cl_2. The reaction was carried out at room temperature. The complex was isolated in a yield of 92%. Anal. Calcd for $C_{49}H_{60}Cl_4P_2Ir_2$: C, 47.57; H, 4.89. Found: C, 47.15; H, 4.82. For NMR data, see Tables 13 and 14. See ref 17 regarding IR data.

$[Cp^*IrCl_2]_2(\mu$-dpph) (13). A 6-mmol (5.6-g) amount of $[Cp^*IrCl_2]_2$ was reacted with a solution of 6 mmol (2.72 g) of dpph in 180 mL of CH_2Cl_2. The reaction was carried out at room temperature. The complex was isolated in a yield of 90%. For NMR data, see Tables 13 and 14. See ref 17 regarding IR data.

$[Cp^*RhCl_2]_2(\mu$-dmpm) (14). A 6-mmol (3.7-g) amount of $[Cp^*RhCl_2]_2$ was reacted with a solution of 6 mmol (0.82 g) of

Table 13. ^{1}H NMR Data of (δ, ppm) for the Complexes [Cp*MCl$_2$]$_2$(μ-P—P) (in CDCl$_3$)

complex	CH$_3$—ring	CH$_3$P	*o*/*p* Ph	*m* Ph	CH$_2$P	CH$_2$CH$_2$P
[Cp*IrCl$_2$]$_2$(μ-dppm) (**8**)	1.38		7.14	7.46	4.80	
[Cp*IrCl$_2$]$_2$(μ-dppe) (**9**)	1.27		7.30	7.46	2.78	
[Cp*IrCl$_2$]$_2$(μ-dppp) (**10**)	1.24		7.30	7.64	2.62	1.56
[Cp*IrCl$_2$]$_2$(μ-dppb) (**11**)	1.27		7.38	7.73	2.56	1.08
[Cp*IrCl$_2$]$_2$(μ-dpppe) (**12**)	1.27		7.37	7.72	2.58	1.06
[Cp*IrCl$_2$]$_2$(μ-dpph) (**13**)	1.42		7.41	7.78	2.77	1.11
[Cp*RhCl$_2$]$_2$(μ-dmpm) (**14**)	1.63	1.80			3.02	
[Cp*RhCl$_2$]$_2$(μ-dmpp) (**15**)	1.61	1.53			2.03	1.76
[Cp*RhCl$_2$]$_2$(μ-dppm) (**16**)	1.27		6.90	7.46	4.64	
[Cp*RhCl$_2$]$_2$(μ-dppp) (**17**)	1.24		7.31	7.69	2.55	1.63
[Cp*RhCl$_2$]$_2$(μ-dppb) (**18**)	1.26		7.42	7.80	2.53	1.07
[Cp*RhCl$_2$]$_2$(μ-dpppe) (**19**)	1.27		7.40	7.79	2.47	1.00
[Cp*RhCl$_2$]$_2$(μ-dpph) (**20**)	1.28		7.42	7.83	2.56	0.95
[(hmb)RuCl$_2$]$_2$(μ-dmpm) (**21**)	1.98	1.66			2.73	
[(hmb)RuCl$_2$]$_2$(μ-dmpp) (**22**)	2.01	1.43			1.60	1.93
[(hmb)RuCl$_2$]$_2$(μ-dmph) (**13**)	2.01	1.37			1.84	1.43

Table 14. ^{13}C{^{1}H} and ^{31}P{^{1}H} NMR Data (δ, ppm) for the Complexes [Cp*MCl$_2$]$_2$(μ-P—P)

	^{13}C NMR									^{31}P NMR
no.	CH$_3$—ring	C ring	CH$_3$P	*i* Ph	*o* Ph	*m* Ph	*p* Ph	CH$_2$P	β-CH$_2$	γ-CH$_2$	P
8	8.3	92.2		128.9	134.7	127.0	130.4	22.6			−5.6
9	8.1	92.0		129.6	134.0	128.0	130.5	22.7			−1.0
10	8.0	91.8		129.8	133.6	127.8	130.2	28.7	19.2		−4.4
11	8.0	91.7		129.1	133.6	128.0	130.5	26.3	25.5		−2.1
12	8.0	91.7		129.6	133.6	127.9	130.4	26.3	23.2	32.1	−2.9
13	8.1	91.8		129.6	133.7	127.9	130.5	26.3	23.7	30.6	−2.6
14	9.2	98.6	13.9					26.0			20.3
15	9.2	98.2	11.7					29.3	18.3		19.7
16	8.7	98.7		129.9	134.6	127.4	131.9	24.4			28.0
17	8.5	96.5		129.7	133.8	127.9	130.3	29.4	19.7		27.4
18	8.5	96.4		131.7	133.8	128.2	130.7	24.1	22.3		30.3
19	8.5	98.3		129.6	133.8	128.1	130.6	27.6	23.5	31.8	29.5
20	8.5	98.4		129.5	133.8	128.1	130.6	27.5	23.9	30.4	29.9
21	24.9	95.1	14.0					24.9			13.9
22	16.0	96.4	12.3					19.7	18.3		7.5
23	16.0	95.3	12.0					28.6	20.9	23.4	7.4

Table 15. Fractional Coordinates and Thermal Parameters for [Cp*IrCl$_2$]$_2$(μ-dmpbe) (7)

atom	*x*	*y*	*z*	*B* (Å^2)[a]	atom	*x*	*y*	*z*	*B* (Å^2)[a]
Ir1	0.72402(2)	0.11229(2)	0.18847(3)	2.221(5)	C17	0.8209(7)	−0.0635(5)	0.298(1)	4.6(2)
Ir2	1.27247(2)	0.41802(2)	0.28792(3)	2.197(5)	C18	0.8625(6)	0.1126(6)	0.5368(9)	3.7(2)
Cl1	0.6239(1)	0.2094(1)	0.0616(3)	3.63(4)	C19	0.6605(6)	0.1888(6)	0.545(1)	4.8(2)
Cl2	0.7416(2)	0.0512(1)	−0.0810(2)	3.64(4)	C20	1.3023(5)	0.4556(5)	0.0410(9)	2.9(2)
Cl3	1.2399(2)	0.5548(1)	0.4030(3)	4.27(5)	C21	1.3921(5)	0.4876(5)	0.1447(8)	2.7(1)
Cl4	1.3071(2)	0.3687(2)	0.5607(2)	3.85(4)	C22	1.4244(5)	0.4152(5)	0.2146(9)	3.0(2)
P1	0.8505(1)	0.2280(1)	0.1567(2)	2.17(3)	C23	1.3580(5)	0.3361(5)	0.1596(9)	3.0(2)
P2	1.1060(1)	0.3706(1)	0.3110(2)	2.26(4)	C24	1.2839(6)	0.3612(5)	0.0475(8)	2.9(2)
C1	0.8533(6)	0.2710(5)	−0.0489(9)	3.3(2)	C25	1.2518(6)	0.5117(5)	−0.0732(9)	3.8(2)
C2	0.8309(5)	0.3155(5)	0.2968(9)	3.0(2)	C26	1.4401(6)	0.5814(5)	0.166(1)	4.1(2)
C3	1.0650(6)	0.3911(5)	0.5140(9)	3.6(2)	C27	1.5154(6)	0.4127(6)	0.331(1)	4.5(2)
C4	1.0416(6)	0.4336(5)	0.167(1)	3.9(2)	C28	1.3751(6)	0.2457(5)	0.196(1)	4.2(2)
C10	0.6037(6)	0.0519(6)	0.3380(9)	3.6(2)	C29	1.2083(6)	0.2996(6)	−0.0598(9)	3.8(2)
C11	0.6466(6)	−0.0158(5)	0.2749(9)	3.4(2)	C30	0.9763(5)	0.2018(5)	0.1981(8)	2.3(1)
C12	0.7519(6)	0.0004(5)	0.3293(9)	3.1(2)	C31	1.0644(5)	0.2516(4)	0.2704(8)	2.4(1)
C13	0.7690(5)	0.0787(5)	0.4349(8)	2.8(2)	C32	1.1419(5)	0.2053(5)	0.3113(9)	3.0(2)
C14	0.6780(6)	0.1126(5)	0.4363(9)	3.2(2)	C33	1.1379(5)	0.1171(5)	0.2713(9)	3.2(2)
C15	0.4965(6)	0.0623(7)	0.315(1)	5.5(2)	C34	1.0565(6)	0.0714(5)	0.186(1)	3.5(2)
C16	0.5974(8)	−0.0939(7)	0.170(1)	6.4(3)	C35	0.9765(5)	0.1133(5)	0.1537(9)	3.0(2)

[a] Anisotropically refined atoms are given in the form of the isotropic equivalent displacement parameters defined as $^4/_3[a^2\beta(1,1) + b^2\beta(2,2) + c^2\beta(3,3) + ab(\cos 99.53°)\beta(1,2) + ac(\cos 93.92°)\beta(1,3) + bc(\cos 91.58°)\beta(2,3)]$.

dmpm in 180 mL of CH_2Cl_2. The reaction was carried out at 0 °C. The complex was isolated in a yield of 99%. For NMR data, see Tables 13 and 14. See ref 17 regarding IR data.

[Cp*RhCl$_2$]$_2$(μ-dmpp) (15). A 6-mmol (3.7-g) amount of [Cp*RhCl$_2$]$_2$ was reacted with a solution of 6 mmol (0.98 g) of dmpp in 180 mL of CH_2Cl_2. The reaction was carried out at 0 °C. The complex was isolated in a yield of 88%. For NMR data, see Tables 13 and 14. See ref 17 regarding IR data.

[Cp*RhCl$_2$]$_2$(μ-dppm) (16). A 6-mmol (3.7-g) amount of [Cp*RhCl$_2$]$_2$ was reacted with a solution of 6 mmol (2.30 g) of dppm in 180 mL of CH_2Cl_2. The reaction was carried out at room temperature. The complex was isolated in a yield of 81%. For NMR data, see Tables 13 and 14. See ref 17 regarding IR data.

[Cp*RhCl$_2$]$_2$(μ-dppp) (17). A 6-mmol (3.7-g) amount of [Cp*RhCl$_2$]$_2$ was reacted with a solution of 6 mmol (2.47 g) of dppp in 180 mL of CH_2Cl_2. The reaction was carried out at room temperature. The complex was isolated in a yield of 58%. For NMR data, see Tables 13 and 14. See ref 17 regarding IR data.

[Cp*RhCl$_2$]$_2$(μ-dppb) (18). A 6-mmol (3.7-g) amount of [Cp*RhCl$_2$]$_2$ was reacted with a solution of 6 mmol (2.56 g) of

Table 16. Fractional Coordinates and Thermal Parameters for [(hmb)$RuCl_2$]$_2$(μ-dmph) (23)

atom	x	y	z	B (Å^2)[a]
Ru1	0.24347(6)	0.79260(4)	0.97804(3)	2.31(1)
Cl1	−0.0164(2)	0.8123(1)	0.9602(1)	3.83(5)
Cl2	0.1875(2)	0.6740(1)	0.8630(1)	4.05(5)
P1	0.1422(2)	0.6909(1)	1.0328(1)	3.45(5)
C1	0.4879(8)	0.8201(4)	1.0264(4)	2.8(2)
C2	0.4071(8)	0.8733(4)	1.0770(4)	2.9(2)
C3	0.3146(8)	0.9268(4)	1.0513(4)	2.9(2)
C4	0.3100(8)	0.9309(4)	0.9763(4)	3.2(2)
C5	0.3860(8)	0.8772(5)	0.9268(4)	3.1(2)
C6	0.4719(8)	0.8194(5)	0.9521(4)	3.1(2)
C7	0.6003(9)	0.7701(5)	1.0550(5)	4.4(2)
C8	0.429(1)	9.8767(5)	1.1580(5)	4.6(2)
C9	0.2253(9)	0.9813(5)	1.1020(5)	4.7(2)
C10	0.213(1)	0.9910(5)	0.9512(5)	5.0(2)
C11	0.369(1)	0.8759(6)	9.8466(5)	5.8(3)
C12	0.554(1)	0.7614(6)	0.8988(5)	5.4(3)
C13	0.270(1)	0.6237(5)	1.0627(5)	4.6(2)
C14	0.3408(9)	0.5689(5)	1.0003(4)	3.8(2)
C15	0.4604(9)	0.5249(5)	1.0305(5)	4.2(2)
C16	−0.016(1)	0.6106(5)	0.9753(5)	5.7(3)
C17	0.065(1)	0.7364(6)	1.1164(5)	5.7(3)

[a] Anisotropically refined atoms are given in the form of the isotropic equivalent displacement parameters defined as $^4/_3[a^2\beta(1,1) + b^2\beta(2,2) + c^2\beta(3,3) + ab(\cos 97.41°)\beta(1,2) + ac(\cos 96.90°)\beta(1,3) + bc(\cos 106.46°)\beta(2,3)]$.

dppb in 180 mL of CH_2Cl_2. The reaction was carried out at room temperature. The complex was isolated in a yield of 95%. For NMR data, see Tables 13 and 14. See ref 17 regarding IR data.

[Cp*$RhCl_2$]$_2$(μ-dppe) (19). A 6-mmol (3.7-g) amount of [Cp*$RhCl_2$]$_2$ was reacted with a solution of 6 mmol (2.64 g) of dpppe in 180 mL of CH_2Cl_2. The reaction was carried out at room temperature. The complex was isolated in a yield of 67%. For NMR data, see Tables 13 and 14. See ref 17 regarding IR data.

[Cp*$RhCl_2$]$_2$(μ-dpph) (20). A 6-mmol (3.7-g) amount of [Cp*$RhCl_2$]$_2$ was reacted with a solution of 6 mmol (2.72 g) of dpph in 180 mL of CH_2Cl_2. The reaction was carried out at room temperature. The complex was isolated in a yield of 60%. For NMR data, see Tables 13 and 14. See ref 17 regarding IR data.

[(hmb)$RuCl_2$]$_2$(μ-dmpm) (21). A mixture of 6.1 mmol (0.83 g) of dmpm and 80 mL of $CHCl_3$ was added dropwise to a solution of 6 mmol (4.0 g) of [(hmb)$RuCl_2$]$_2$ in 600 mL of $CHCl_3$ over 1 h at 0 °C. The orange-red solution is stirred for 18 h. A 450-mL amount of the solvent is evaporated, and when 250 mL of *n*-pentane is added, a red solid precipitates, which is isolated by filtration. The complex was isolated in a yield of 60%. For NMR data, see Tables 13 and 14. See ref 17 regarding IR data.

[(hmb)$RuCl_2$]$_2$(μ-dmpp) (22). By the procedure for **21**, 6 mmol (3.7 g) of [(hmb)$RuCl_2$]$_2$ was reacted with a solution of 6.1 mmol (1.00 g) of dmpp in 80 mL of $CHCl_3$. The complex was isolated in a yield of 68%. For NMR data, see Tables 13 and 14. See ref 17 regarding IR data.

[(hmb)$RuCl_2$]$_2$(μ-dmph) (23). By the procedure for **21**, 6 mmol (3.7 g) of [(hmb)$RuCl_2$]$_2$ was reacted with a solution of 6.1 mmol (1.32 g) of dmpp in 80 mL of $CHCl_3$. The complex was isolated in a yield of 65%. For NMR data, see Tables 13 and 14. See ref 17 regarding IR data. The X-ray structure is shown in Figure 4, and crystal data are given in Table 5. Table 16 lists the data obtained for the fractional coordinates.

[Cp*$Ir(H)_2$]$_2$(μ-dmpe) (24). A 114-mg (0.12-mmol) amount of **1** was suspended in 16 mL of diethyl ether and cooled to 0 °C. To this suspension was added 6 equiv (0.72 mmol) of a 1 M Super-Hydride THF solution (Li(Et_3BH)] dropwise. After 4 h of stirring at 0 °C, the reaction mixture was filtered over a 1−2 cm thick layer of silica (70−270 mesh). Evaporation to dryness of the brownish solution gave 38.8 mg (40%) of the hydride complex **24**. Further purification was carried out by column chromatography with diethyl ether at 0 °C on silica. The overall yield is about 20%. ^{1}H NMR (C_6D_6): δ −17.57 (d, $^2J_{HP}$ = 31.3 Hz, Ir($H)_2$), 1.35 (x, $(CH_3)_2PCH_2$), 1.70 (d, $^2J_{HP}$ = 1.6 Hz, $(CH_3)_2PCH_2$), 2.12 ppm (s, η^5-$C_5(CH_3)_5$). ^{13}C NMR (C_6D_6): δ 11.7 (s, η^5-$C_5(CH_3)_5$), 21.7 (dd, $^1J_{HP}$ = 18.1 Hz, $^4J_{HP}$ = 18.1 Hz, $(CH_3)_2PCH_2$), 32.0 (dd, $^1J_{HP}$ = 17.6 Hz, $^2J_{HP}$ = 17.6 Hz, $(CH_3)_2PCH_2$), 91.5 ppm (s, η^5-$C_5(CH_3)_5$). ^{31}P NMR (C_6D_6): δ −28.8 ppm (s). IR [ν, cm^{-1}): 2970, 2959, 2903, 2115, 2086, 1630, 1469, 1450, 1424, 1410, 1380, 1289, 1278, 1261, 1164, 1076, 1030, 855, 840, 821, 800, 737, 723, 711, 700, 673, 614, 428, 410. UV (cyclohexane): λ 221 (ε = 2000), 264 nm (ε = 9500).

[(hmb)$Ru(H)_2$]$_2$(μ-dmpe) (25). A 164-mg (0.2-mmol) amount of **3** and 72.9 mg (1.9 mmol) of $NaBH_4$ were suspended in 15 mL of ^{i}PrOH. The reaction mixture was refluxed for 3 h, cooled to room temperature, and filtered over a 2−3-cm layer of silica gel (70−230 mesh). Evaporation to dryness yielded 48 mg (35% based on **3**). ^{1}H NMR (C_6D_6): δ −11.12 (d, $^2J_{HP}$ = 47.2 Hz, Ru($H)_2$), 1.18 (x, $(CH_3)_2PCH_2$), 1.58 (s, $(CH_3)_2PCH_2$), 2.18 ppm (s, η^6-$C_6(CH_3)_6$). ^{13}C NMR (C_6D_6): δ 18.5 (s, η^6-$C_6(CH_3)_6$), 22.9 (x, $(CH_3)_2PCH_2$), 32.9 (x, $(CH_3)_2PCH_2$), 95.3 ppm (s, η^6-$C_6(CH_3)_6$). ^{31}P NMR (C_6D_6): δ 23.6 ppm (s). IR (ν, cm^{-1}): 3010, 2980, 2965, 2930, 2910, 1928, 1895, 1640, 1420, 1420, 1375, 1285, 1275, 1165, 1075, 1015, 950, 900, 855, 830, 800, 727, 705, 695, 687, 667, 550, 533, 423.

Acknowledgment. We thank the Koninklijke/Shell-Laboratorium, Amsterdam (Shell Research BV), for generous support of this work and the Degussa AG, Frankfurt, Germany, for providing the noble metals.

Supplementary Material Available: Tables of bond lengths and angles, positional parameters, and anistropic thermal parameters for **2**, **4**, **5**, **7**, and **23** and a table of torsion angles for **23** (52 pages). Ordering information is given on any current masthead page.

OM930387X